

# Influence of Turbulence Modeling on Predictions of Turbulent Combustion

Inge R. Gran,\* Ivar S. Ertesvåg,<sup>†</sup> and Bjørn F. Magnussen<sup>‡</sup>  
Norwegian University of Science and Technology, N-7034 Trondheim, Norway

Computations of an axisymmetric bluff-body stabilized turbulent diffusion flame are presented. The effects of turbulence modeling on turbulent combustion predictions are studied. The test case is simulated using  $k-\varepsilon$  and Reynolds-stress-equation turbulence models with and without extensions for low Reynolds numbers. Turbulent combustion is modeled by two different combustion models with fast chemistry. Effects of chemical kinetics are studied by including detailed chemistry in one combustion model. The combustion predictions are considerably affected by the choice of turbulence model. The nonpremixed flame is stabilized by a recirculation zone behind the bluff body. In isothermal, nonreacting flow, the predictions of the recirculation zone are quite similar for the four models. With combustion, a Reynolds-stress-equation closure predicts a significantly weaker recirculation compared with the  $k-\varepsilon$  results. This allows a larger spreading of the fuel and better mixing in the bluff-body wake. When finite-rate chemistry is introduced, the  $k-\varepsilon$  model predicts blow out, whereas the Reynolds-stress-equation model does not. This is due to the larger spreading and mixing by the latter model. The low-Reynolds-number extensions gave a much too strong recirculation, which reduced the spreading of the fuel jet.

## Introduction

FOR numerical simulations of turbulent reacting flows, one has to choose a model for the turbulent fluid flow, a model for the interaction between turbulence and combustion, models for chemistry and thermodynamics, numerical procedures, and so on. A successful prediction depends on all of these factors.

The objective of this study is to investigate the influence of the turbulence model on combustion calculations. We want to see how the combustion prediction is affected when a turbulence model is replaced by another.

Turbulent jet diffusion flames have been studied at length because they are simple enough to represent by eddy-viscosity models, to be described by the parabolic form of the governing equations, and to permit advanced laser-based spectroscopic measurements.<sup>1</sup> A major drawback of the jet flames is the low turbulence level that can be achieved before the flame is blown off for laboratory-scale flames. A test case with a more complex flow is desired.

## Test Case

In the drive towards experiments with strong turbulence-chemistry interactions, a bluff-body stabilized CO/H<sub>2</sub>/N<sub>2</sub> burner has been studied experimentally by Correa and Gulati.<sup>2</sup> It was possible to operate this burner in a regime without unsteadiness in the mean flow. The advantage of this flow is the high turbulence dissipation rate that can be achieved.

Correa and Gulati<sup>2</sup> reported measurements of temperature and major species mass fractions. Values of the mean mixture fraction  $\bar{f}$  and the normalized fluctuation intensity of the mixture fraction  $f'/\bar{f}$  were deduced from the species concentrations. The fluctuation intensity was defined as the rms of the fluctuation  $f' = (\overline{f'^2})^{1/2}$ .

Localized extinction was not observed at any axial location in the scatter plots. Unfortunately, there are no reported measurements of the mean or fluctuating velocity or pressure fields for this flow.

The fuel-jet diameter was  $d = 3.18$  mm, the bluff body extended radially to  $r/d = 6$ , and the computational domain extended axially

to  $x/d = 55$ . The fuel-jet velocity was 80 m/s, and the air inlet velocity was 6.5 m/s. The burner pressure was 101 kPa, and the inlet temperatures were 300 K. The syngas fuel consisted of 27.5% CO, 32.3% H<sub>2</sub>, and 40.2% N<sub>2</sub> by volume. The inlet Reynolds numbers based on diameters were  $5.8 \times 10^3$  for the fuel jet and  $4.77 \times 10^4$  for the coflowing air.

The mixture fraction was defined as one in the fuel stream and zero in the coflowing air. The stoichiometric mixture fraction for this mixture was  $f_{st} = 0.323$ , and the stoichiometric equilibrium temperature was 2181 K.

Figure 1 shows the burner with predicted temperature contours and streamlines of the flow. The fuel, syngas, is injected as a central jet in a wind tunnel. An important region of the flow is the base of the jet where the flame is stabilized by a recirculation bubble.

The paper by Correa and Gulati<sup>2</sup> also reported predictions based on an assumed probability density function (PDF) model and the  $k-\varepsilon$  turbulence model. Simulations of the flame have also been conducted by Correa et al.<sup>3</sup> They employed a hybrid model, which combined the  $k-\varepsilon$  model and a joint scalar-velocity PDF transport model.

## Turbulence Models

The system of Favre-averaged transport equations is closed by four different turbulence models: 1) the standard  $k-\varepsilon$  model<sup>4</sup> for flows at high Reynolds numbers, 2) the Reynolds-stress-equation (RSE) model for flows at high Reynolds numbers (Basic Model),<sup>5</sup> 3) the low-Reynolds-number  $k-\varepsilon$  model by Launder and Sharma,<sup>6</sup> and 4) the low-Reynolds-number RSE model by Kebede et al.<sup>7</sup>

The first two models are in widespread use and can be regarded as standard models for industrial-flow calculations. The latter two contain easy-to-implement extensions and also have been used in many cases, especially the  $k-\varepsilon$  version. More advanced models exist, but they are still under development and have not been tested for so many types of flow.

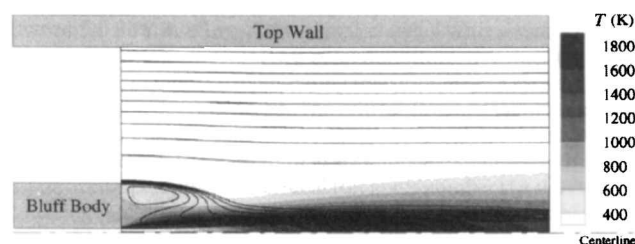


Fig. 1 Temperature contours and streamlines.

Received Nov. 20, 1995; revision received Aug. 26, 1996; accepted for publication Sept. 10, 1996; also published in *AIAA Journal on Disc*, Volume 2, Number 1. Copyright © 1996 by the American Institute of Aeronautics and Astronautics, Inc. All rights reserved.

\*Research Fellow, Department of Applied Mechanics, Thermodynamics, and Fluid Dynamics.

<sup>†</sup>Associate Professor, Department of Applied Mechanics, Thermodynamics, and Fluid Dynamics.

<sup>‡</sup>Professor, Head of Department, Department of Applied Mechanics, Thermodynamics, and Fluid Dynamics.

For all models, wall functions are used at the solid surfaces. The low-Reynolds-number models have also been tested with full integration onto the bluff body. For the scalar transport, the gradient-diffusion model is used. The turbulence models are the same as used for constant-density flows, except that the divergence term is nonzero in the turbulence-viscosity stress model and in the turbulence-energy production term.

A known weakness of the  $k$ - $\varepsilon$  turbulence model is the prediction of recirculation zones. RSE models generally predict recirculation with better accuracy. The jet flame in the test case is stabilized by a recirculation zone. It is therefore interesting to study the predicted flow pattern in the wake behind the bluff body. These models, with standard values for model constants, are also known to overpredict the spread rate of axisymmetric jets by about 10%. However, we regard this as a minor issue compared with the prediction of recirculation zones.

### Combustion Models

Since Favre-averaged transport equations are used, closure for the mean reaction rate in the transport equations for species mass fractions is needed.

The following models have been employed in this study: 1) the assumed-PDF method with a fast-chemistry assumption,<sup>8</sup> 2) the Eddy-Dissipation Concept (EDC) by Magnussen,<sup>9</sup> with a fast-chemistry assumption, and 3) the EDC with detailed chemistry.

When fast chemistry is assumed, the difficulty associated with closure of the mean reaction rate can be avoided by relating the instantaneous composition to a conserved scalar such as the mixture fraction. This has been done in the assumed-PDF method. The PDF of the mixture fraction is assumed to be a normalized beta function. The two parameters in the beta function are determined by solving modeled transport equations for the mean and the variance of the mixture fraction.

An important assumption in the EDC is that most of the reactions occur in the smallest scales of the turbulence (the fine structures). When fast chemistry is assumed, the state in the fine structures is taken as equilibrium. In the detailed chemistry calculations, the fine structures are treated as well-stirred reactors. The reactor computations are carried out using the ordinary differential equation solver LIMEX by Deuffhard et al.<sup>10</sup> The CO/H<sub>2</sub>/air mechanism is taken from Maas and Warnatz<sup>11</sup> and consists of 13 species and 67 reactions.

The method for evaluating the temperature depends on which combustion model is being used. In any case, polynomial fits<sup>12</sup> are employed for finding the temperature-dependent total enthalpy  $h_i(T)$  for a chemical species  $i$ .

When the EDC model is used, a model equation for the mean total enthalpy  $\tilde{h}$  is solved together with the model equations for the species mass fractions  $\tilde{Y}_i$ . When radiation is neglected, the total enthalpy is assumed to be the same in the reacting turbulent fine structures and the surrounding fluid. The temperature in each of these regions is found by solving the equation

$$\sum Y_i h_i(T) = \tilde{h} \quad (1)$$

for temperature by using Newton–Raphson iteration. The mean temperature can then be found from

$$\tilde{T} = Y^* T^* + (1 - Y^*) T^\circ \quad (2)$$

where  $Y^*$  is the mass fraction of reacting turbulent fine structure<sup>9</sup> and  $T^*$  and  $T^\circ$  denote the temperature of the fine structures and the surroundings, respectively.

In the case of the assumed-PDF method, the temperature is not needed during the flow calculations and is therefore computed when a converged solution has been found. By assumption, the instantaneous temperature is uniquely determined by the mixture fraction  $f$ . The temperature can then be found from

$$\tilde{T} = \int_0^1 T(f) \tilde{p}(f) df \quad (3)$$

With EDC, the dynamic molecular viscosity is calculated as a function of the local temperature and the local composition of the

mixture. With the assumed-PDF method, the viscosity is calculated by

$$\tilde{\mu} = \int_0^1 \mu(f) \tilde{p}(f) df \quad (4)$$

### Numerical Solution

The mathematical models described earlier have been implemented in the general-purpose computational fluid dynamics code SPIDER, developed by Melaaen<sup>13</sup> for calculating fluid flow in complex geometries. This program is based on the finite volume concept and uses a nonorthogonal curvilinear computational mesh with collocated variable arrangement. The convective terms are discretized by the second-order upwind scheme. The pressure field is found by the SIMPLE algorithm. A close coupling between pressure and convective velocity is achieved by the Rhie and Chow interpolation method. The RSEs are solved by the method of Obi et al.<sup>14</sup> The set of algebraic equations that results from the implicit time discretization is solved sequentially with line-by-line tridiagonal-matrix algorithm. The solution is regarded as converged when the one-norm of the residuals scaled against a representative flux is small (typically  $10^{-5}$ ) for all variables.

All calculations presented here are carried out with a  $75 \times 75$  cell grid. Grid dependence was assessed by comparing results based on two different spatial grids. In addition, two different discretization schemes for the convective terms were compared. The variation among these different numerical solutions was negligible compared with those resulting from the different mathematical models.<sup>15</sup>

The results are not significantly affected by the airflow inlet profiles and outer wall position. There is, however, some dependence on the fuel-jet inlet profile for turbulence quantities. This is not a serious problem since the fuel pipe length is much longer than its diameter. Hence, it is likely that the fully developed flow is a reasonable assumption for the fuel jet.<sup>15</sup> Various near-wall treatments (wall functions and full integration) at the bluff body for the low-Reynolds-number models do not affect the result.

### Reacting and Nonreacting Flow

First, the test case was calculated with air also in the central jet. For this isothermal, constant-density flow, the  $k$ - $\varepsilon$  model and the RSE model predict recirculation bubbles extending approximately to 5.0 and 5.2 jet diameters, respectively. Introducing low-Reynolds-number extensions gives only small changes. In the literature, the lengths of recirculation zones are often used as a parameter for comparing different models. The models tested here are quite similar in this instance.

For the isothermal mixing of fuel and air without reaction, the predicted bubbles are approximately 5.5 and 5.6 jet diameters long. The predicted streamlines for the mixing calculations are shown in Figs. 2a and 2b. Low-Reynolds-number extensions of the models give only moderate changes to these results. Now the recirculation bubbles extend to 6.2 and 6.3 jet diameters. The predicted turbulence Reynolds number,  $R_T = \rho k^2 / (\mu \varepsilon)$ , is high in most parts of the flow.

All experimental data are for reacting flow. There are no corresponding measurements for non-reacting flows.

For the reacting flow two important differences appear in the predictions.

1) There is a substantial difference between  $k$ - $\varepsilon$  and RSE models (see the following text).

2) The turbulence Reynolds number  $R_T$  is reduced. This leads to large changes when low-Reynolds-number extensions are applied to the models.

### Results with Fast-Chemistry Assumption

#### Combustion Models

In the following, results from the EDC predictions are presented. Results from the assumed-PDF method were very close to the EDC results for all of the different turbulence models and are not shown.

#### High-Reynolds-Number Turbulence Models

In the predictions, the recirculation bubble extends to 8.5 jet diameters ( $x/d$ ) downstream from the inlets. The recirculation bubble

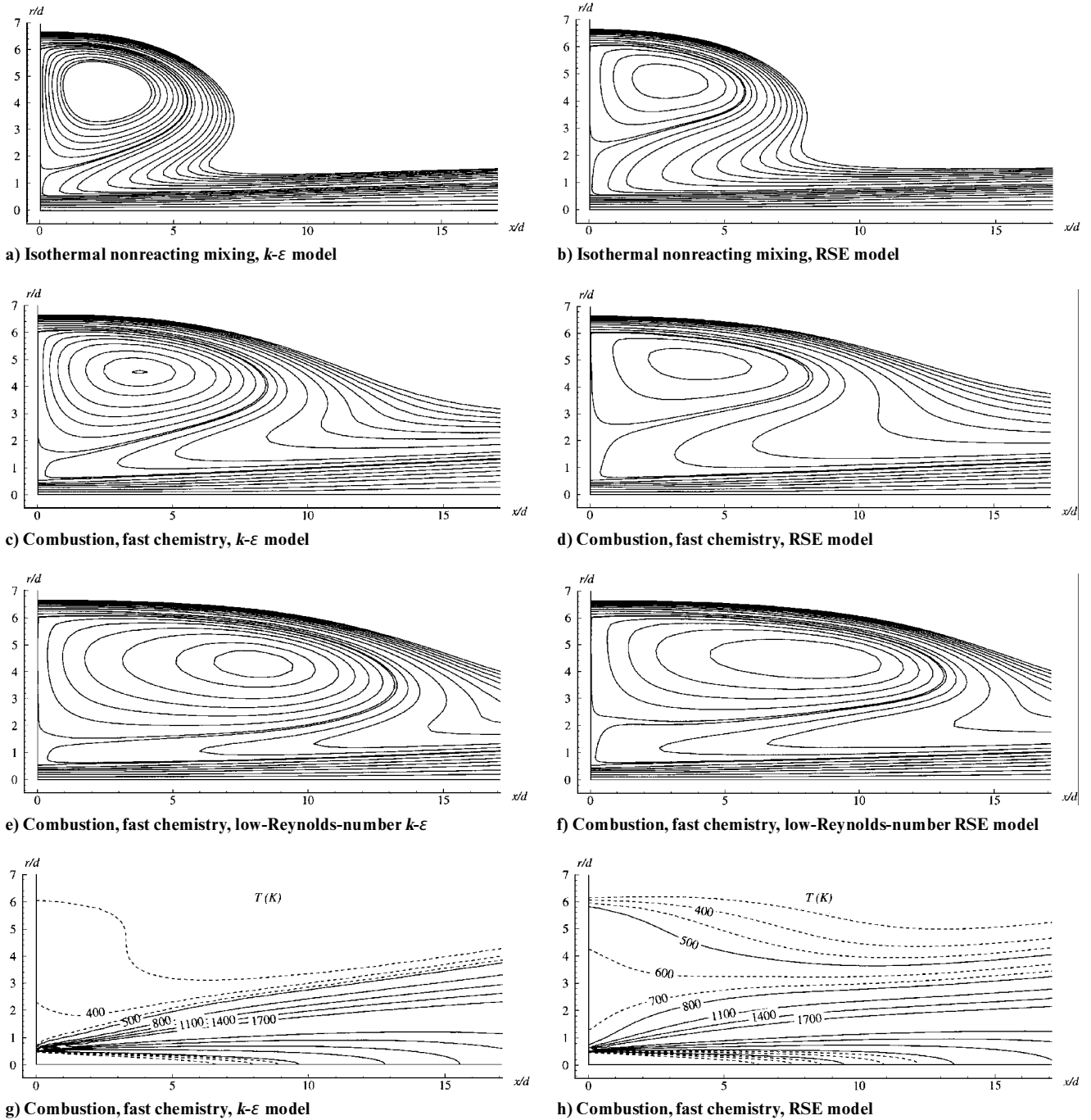


**Fig. 2** Predicted streamlines and temperature contours in the vicinity of the bluff body. Streamlines are not equidistant but have the same values in all panels.

establishes a hot region at the fuel-jet entrance. Close to the wind-tunnel wall, however, the flow is largely unaffected by the bluff body and the flame. For example, the computed mass fraction originating from the fuel jet at the exit of the computational domain ( $x/d = 55$ ) is zero less than halfway from the centerline to the wind-tunnel wall. Figures 2c and 2d compare the streamlines predicted by the two turbulence models.

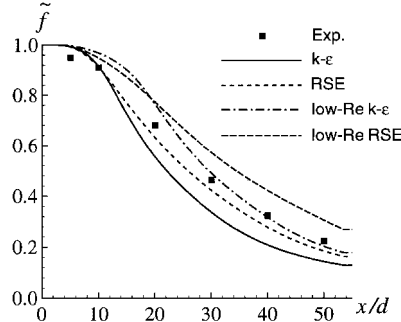
The predicted recirculation bubbles have approximately the same size and shape in the  $k$ - $\varepsilon$  and RSE results. Further, the predicted eddy viscosity in the shear layer between the fuel jet and the recirculation bubble is approximately the same for the two models. However, the circulating flow rates within the recirculation zone, which can be determined from the distance between the streamlines, are far greater in the  $k$ - $\varepsilon$  model results. This strongly influences the amount of matter originating from the fuel jet that is able to diffuse into the recirculation bubble. This can be clearly seen in the temperature

contours shown in Figs. 2g and 2h. These contours also represent the spreading of combustion products. Because of the much lower flow velocities in the RSE results, a significantly higher temperature level is predicted in the wake behind the bluff body.

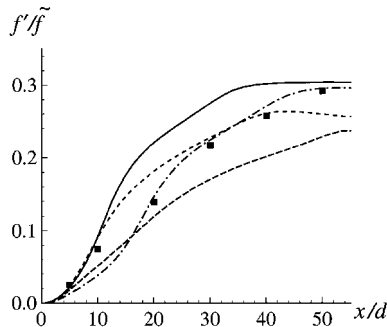
In Fig. 3, axial profiles of the (Favre) mean and normalized fluctuation intensity of the mixture fraction are shown. The predicted axial development of the mean mixture fraction based on the  $k$ - $\varepsilon$  turbulence model is very similar to previous calculations based on the  $k$ - $\varepsilon$  model and an assumed-shape PDF.<sup>2</sup> As expected, the jet decays too fast in the  $k$ - $\varepsilon$  model predictions. The mean mixture-fraction profile based on the RSE model is in better accordance with the Raman data, but also here a too rapid decay of the jet is predicted. The difference in spreading rate is due to different influences from the recirculation zone. The normalized mixture-fraction fluctuation intensity is almost twice the measured value at  $x/d = 20$  in the  $k$ - $\varepsilon$  calculations. This is mainly because the mean value is underpredicted by

the  $k-\varepsilon$  model, but in addition, the calculated variance (not shown) is higher in the  $k-\varepsilon$  results than in the RSE results up to an axial position of  $x/d = 25$ . On the other hand, the RSE results predict too low values for the fluctuation intensity farther downstream.

Figure 4 shows predicted radial profiles of mean mixture fraction and normalized rms of the fluctuating mixture fraction at axial locations of  $x/d = 10, 20$ , and  $40$ . At  $x/d = 10$ , the  $k-\varepsilon$  model and the RSE model results are quite similar for the mean mixture fraction. Also here, we see that both models predict a too rapid spread of the jet. The measured mean values are lower than the RSE results at all radial positions and outside  $r/d = 0.6$  for the  $k-\varepsilon$  results.



a) Mean mixture fraction



b) Normalized rms of mixture fraction

Fig. 3 Axial profiles of mixture fraction. Comparison of predicted results based on the  $k-\varepsilon$  model and the RSE model with Raman data of Correa and Gulati.<sup>2</sup>

Between  $r/d = 2$  and  $5$ , the  $k-\varepsilon$  model is in relatively good agreement with the measured mean mixture fraction, whereas the RSE model overpredicts the spread rate. This discrepancy is attributed to the significantly different flow velocities in the recirculation zone predicted by the two models, which we observed earlier from Figs. 2c and 2d. The mixture-fraction profiles predicted by the  $k-\varepsilon$  model are in quite good agreement with the previous calculations of Correa and Gulati.<sup>2</sup> The normalized fluctuation intensity of the mixture fraction at  $x/d = 10$  is significantly different in the  $k-\varepsilon$  and RSE results. The reason for this is mainly the lower mean values predicted by the  $k-\varepsilon$  model outside  $r/d = 2$ . The agreement between the measured and calculated values is good up to  $r/d = 3$ , especially in the RSE results. Outside this radius, the results are very sensitive to the mean value. Radial mixture fraction profiles at axial position  $x/d = 20$  are shown in Figs. 4c and 4d. Here, the predicted mean values differ significantly between the  $k-\varepsilon$  and the RSE model. The  $k-\varepsilon$  model predicts a too rapid spread of the jet. Also the RSE model overpredicts the spread rate but to a much lesser extent. There are no available measurements of the normalized fluctuation intensity at this axial position.

Figures 4e and 4f show predicted radial profiles of mean and normalized rms of mixture fraction at axial location  $x/d = 40$ . At  $x/d = 40$  there are no measured values for the mean mixture fraction. In the calculation, the  $k-\varepsilon$  model still predicts a higher spread rate than the RSE model. The normalized fluctuation intensity is well predicted by the RSE model. The difference between the  $k-\varepsilon$  and RSE results is mainly due to the difference in predicted mean value.

#### Low-Reynolds-Number Turbulence Models

Contrary to the nonreacting case, the low-Reynolds-number extensions have a large influence on the combustion results. The streamlines are shown in Figs. 2e and 2f for  $k-\varepsilon$  and RSE models, respectively. The recirculation bubble now extends to more than 13 jet diameters downstream. In Figs. 3 and 4, it can be seen that the decay and spreading of the central jet are much slower.

In the hottest part of the flame, the dynamic viscosity is increased 3 to 5 times compared with the cold fluid. The density is reduced by a factor of 3 to 4. That is, because of the temperature, the kinematic viscosity is increased, at the most by a factor of 10 to 20. The turbulence Reynolds number  $Re_T$  is decreased by the same factor.

The low-Reynolds-number models contain an extra production term in the  $\varepsilon$ -equation. This term is proportional to the square of

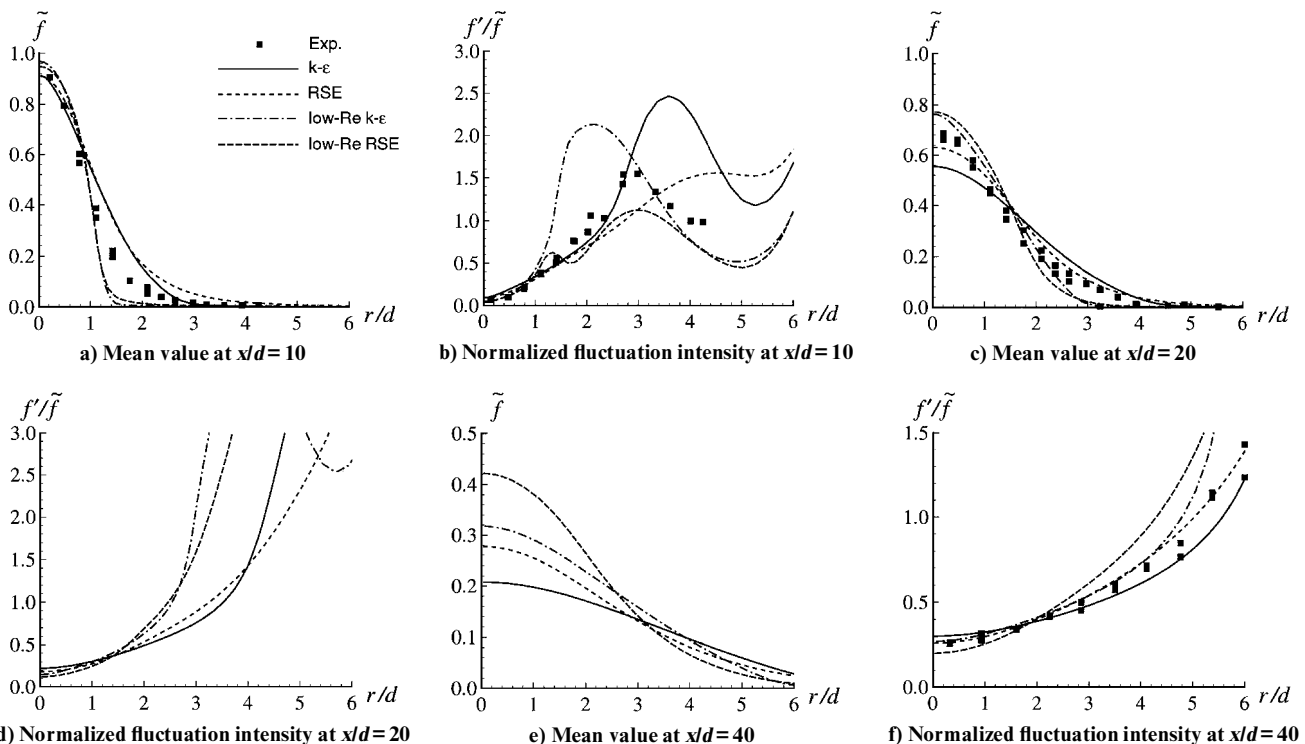


Fig. 4 Radial profiles of mixture fraction at axial locations  $x/d = 10, 20$ , and  $40$ . Comparison of predicted results based on the  $k-\varepsilon$  model and the RSE model with Raman data of Correa and Gulati.<sup>2</sup>

the second derivative of the mean velocity. The increased dissipation reduces turbulence velocities. Turbulence transport is modeled proportional to the time scale  $k/\varepsilon$  and is reduced by the extra  $\varepsilon$  production. Furthermore, the turbulence Reynolds number is decreased by the reduced  $k$  and enhanced  $\varepsilon$ .

The reduced shear allows the recirculation against the jet to be stronger. The reduced transport also causes less fuel and combustion products to be brought into the airflow. The spreading of the fuel and combustion products, and thus the spreading of the temperature field, is less than shown for the standard  $k$ - $\varepsilon$  model in Fig. 2g.

The introduction of the low-Reynolds-number extensions showed very poor results for the present test case. The models are developed for nearly isothermal, constant-density flows. The results indicate that such models cannot necessarily be used in combustion calculations.

### Results with Finite-Rate Chemistry

The absence of local extinction in this flow limits the errors associated with the fast-chemistry assumption. Nevertheless, the temperature mixture-fraction scattergrams from the measurements<sup>2</sup> show departure from equilibrium at axial positions  $x/d = 5$  and 10. In addition, the measured temperature profiles at both  $x/d = 10$  and 20 do not fit the measured  $H_2O$  profiles if fast chemistry is assumed. The effects of finite-rate chemical kinetics in this flame have been studied by computing the fine structures in the EDC model with detailed chemistry.<sup>15</sup>

Predictions are performed based on the  $k$ - $\varepsilon$  model and the RSE model. The  $k$ - $\varepsilon$  model predicts blowout, whereas the RSE model does not.

This can be understood by looking at the fast-chemistry results in Figs. 2c, 2d, 2g, and 2h again. The predicted recirculation zone behind the bluff body does not transport enough combustion products back to the base of the fuel jet to anchor the flame when finite-rate chemistry is introduced in the  $k$ - $\varepsilon$  calculations. In the RSE calculations, however, the temperature behind the bluff body is much higher, and the flame is stabilized. This is a remarkable finding, which underscores the importance of turbulence modeling in the study of chemical kinetics in turbulent combustion.

### Concluding Remarks

An axisymmetric bluff-body stabilized turbulent diffusion flame is studied. Measurements of major species mass fractions and temperature have been reported in the literature. Local extinction was not observed in the measurements.

Predictions of the flame are carried out using two different turbulence models with and without low-Reynolds-number extensions.

The RSE model predicts a spread rate of the fuel jet in better accordance with the measurements than the  $k$ - $\varepsilon$  model.

In nonreacting flow, low-Reynolds-number extensions do not affect the calculations very much. Combustion calculations are, however, strongly affected. Low-Reynolds-number extensions to the turbulence models cause turbulent transport to be underpredicted. This gives too slow decay and too weak spreading of the jet and the flame.

Fast-chemistry calculations have been carried out with two different combustion models: Magnussen's EDC and the assumed-PDF method. For the different turbulence models, there are only small differences between the results from the two combustion models.

The effects of chemical kinetics are studied by including detailed chemistry into the EDC model. The flame is stabilized when the RSE model is employed, whereas the  $k$ - $\varepsilon$  model predicts blowout.

### Acknowledgment

I. R. Gran is grateful for financial support from the Norwegian Research Council.

### References

- <sup>1</sup>Correa, S. M., and Shyy, W., "Computational Models and Methods for Continuous Gaseous Turbulent Combustion," *Progress in Energy and Combustion Science*, Vol. 13, No. 3, 1987, pp. 249–292.
- <sup>2</sup>Correa, S. M., and Gulati, A., "Measurements and Modeling of a Bluff Body Stabilized Flame," *Combustion and Flame*, Vol. 89, No. 2, 1992, pp. 195–213.
- <sup>3</sup>Correa, S. M., Gulati, A., and Pope, S. B., "Raman Measurements and Joint pdf Modeling of a Premixed Bluff-Body-Stabilized Methane Flame," *25th Symposium (International) on Combustion*, Combustion Inst., Pittsburgh, PA, 1994, pp. 1167–1173.
- <sup>4</sup>Launder, B. E., and Spalding, D. B., "The Numerical Computation of Turbulent Flows," *Computer Methods in Applied Mechanics and Engineering*, Vol. 3, 1974, pp. 269–289.
- <sup>5</sup>Launder, B. E., "Second-Moment Closure: Present . . . and Future?" *International Journal of Heat and Fluid Flow*, Vol. 10, No. 4, 1989, pp. 282–300.
- <sup>6</sup>Launder, B. E., and Sharma, B. I., "Application of the Energy-Dissipation Model of Turbulence to the Calculation of Flow near a Spinning Disc," *Letters in Heat and Mass Transfer*, Vol. 1, No. 2, 1974, pp. 131–138.
- <sup>7</sup>Kebede, W., Launder, B. E., and Younis, B. A., "Large-Amplitude Periodic Pipe Flow: A Second-Moment Closure Study," *Proceedings of the 5th Symposium on Turbulent Shear Flows*, Cornell Univ., Ithaca, NY, 1985, pp. 16.23–16.29.
- <sup>8</sup>Bilger, R. W., "Turbulent Flows with Nonpremixed Reactants," *Turbulent Reacting Flows*, Springer-Verlag, Heidelberg, Germany, 1980, pp. 65–113.
- <sup>9</sup>Magnussen, B. F., "Modeling of Pollutant Formation in Gas Turbine Combustors Based on the Eddy Dissipation Concept," *18th International Congress on Combustion Engines*, International Council on Combustion Engines, Tianjin, PRC, 1989.
- <sup>10</sup>Deufhard, P., Hairer, E., and Zguck, J., "One-Step and Extrapolation Methods for Differential-Algebraic Systems," *Numerische Mathematik*, Vol. 51, No. 5, 1987, pp. 501–516.
- <sup>11</sup>Maas, U., and Warnatz, J., "Ignition Processes in Carbon-Monoxide-Hydrogen-Oxygen Mixtures," *22nd Symposium (International) on Combustion*, Combustion Inst., Pittsburgh, PA, 1988, pp. 1695–1704.
- <sup>12</sup>Kee, R. J., Rupley, F. M., and Miller, J. A., "The Chemkin Thermodynamic Data Base," Sandia National Labs., Sandia Rept. SAND87-8215, Livermore, CA, April 1980.
- <sup>13</sup>Melaen, M. C., "Calculation of Fluid Flows with Staggered and Non-staggered Curvilinear Nonorthogonal Grids—The Theory," *Numerical Heat Transfer B*, Vol. 21, No. 1, 1992, pp. 1–19.
- <sup>14</sup>Obi, S., Perić, M., and Scheuerer, G., "Second-Moment Calculation Procedure for Turbulent Flows with Collocated Variable Arrangement," *AIAA Journal*, Vol. 29, No. 4, 1991, pp. 585–590.
- <sup>15</sup>Gran, I. R., "Mathematical Modeling and Numerical Simulation of Chemical Kinetics in Turbulent Combustion," Ph.D. Thesis, Dept. of Applied Mechanics, Thermodynamics, and Fluid Dynamics, Norwegian Inst. of Technology, Trondheim, Norway, 1994.